Simultaneous field-aligned currents at Swarm and Cluster satellites

Dunlop, M. W.; Yang, J. Y.; Yang, Y. Y.; Xiong, C.; Lühr, H.; Bogdanova, Y. V.; Shen, C.; Olsen, N.; Zhang, Q. H.; Cao, J. B.

Published in:
Geophysical Research Letters

Link to article, DOI:
10.1002/2015GL063738

Publication date:
2015

Document Version
Publisher's PDF, also known as Version of record

AGU PUBLICATIONS

Geophysical Research Letters

RESEARCH LETTER
10.1002/2015GL063738

Key Points:
- Gives correlated FAC signatures between low (~500 km) and high (~4 RE) altitudes
- Resolves large- and small-scale structures at low altitude
- Confirms the scaling of current strength at each location

Correspondence to:
M. W. Dunlop,
m.w.dunlop@rl.ac.uk

Citation:
Dunlop, M. W., et al. (2015), Simultaneous field-aligned currents at Swarm and Cluster satellites, *Geophys. Res. Lett.*, *42*, 3683–3691, doi:10.1002/2015GL063738.

Received 4 MAR 2015
Accepted 27 APR 2015
Accepted article online 29 APR 2015
Published online 23 MAY 2015

Simultaneous field-aligned currents at Swarm and Cluster satellites

M. W. Dunlop[1,2,3], J.-Y. Yang[1,4], Y.-Y. Yang[5,6], C. Xiong[7], H. Lühr[7], Y. V. Bogdanova[2], C. Shen[5], N. Olsen[8], Q.-H. Zhang[9], J.-B. Cao[1], H.-S. Fu[1], W.-L. Liu[1], C. M. Carr[3], P. Ritter[7], A. Masson[10], and R. Haagmans[10]

[1]Space Science Institute, School of Astronautics, Beihang University, Beijing, China, [2]RAL_Space, STFC, Chilton, UK, [3]The Blackett Laboratory, Imperial College London, London, UK, [4]Key Laboratory of Earth and Planetary Physics, Chinese Academy of Sciences, Beijing, China, [5]State Key Laboratory of Space Weather, NSSC, Chinese Academy of Sciences, Beijing, China, [6]College of Earth Science, University of Chinese Academy of Sciences, Beijing, China, [7]GFZ, Potsdam, Germany, [8]DTU Space, Lyngby, Denmark, [9]CSW, Institute of Space Sciences, Shangdong University, Weihai, China, [10]ESA/ESTEC, Noordwijk, Netherlands

Abstract We show for the first time, with direct, multispacecraft calculations of electric current density, and other methods, matched signatures of field-aligned currents (FACs) sampled simultaneously near the ionosphere at low (~500 km altitude) orbit and in the magnetosphere at medium (~2.5 R_E altitude) orbits using a particular Swarm and Cluster conjunction. The Cluster signatures are interpreted and ordered through joint mapping of the ground/magnetospheric footprints and estimation of the auroral zone boundaries (taken as indication of the boundaries of Region 1 and Region 2 currents). We find clear evidence of both small-scale and large-scale FACs and clear matching of the behavior and structure of the large-scale currents at both Cluster and Swarm. The methodology is made possible through the joint operations of Cluster and Swarm, which contain, in the first several months of Swarm operations, a number of close three-spacecraft configurations.

1. Introduction

The Earth's ring current and large-scale (R1/R2) field-aligned currents (FACs) have been studied for many decades and represent the dominant influence on the geomagnetic field and on the transport of energy and momentum, respectively. FACs, in particular, are therefore fundamentally important for an understanding of magnetosphere-ionosphere coupling, yet until recently, have not been directly spatially measured, although signatures of FACs have been extensively reported [*McPherron et al.*, 1973; *Shiokawa et al.*, 1998; *Cao et al.*, 2010]. In addition, the form of the FACs, flowing along near-Earth field lines, has a highly time-dependent signature, depending on their scale size, so that separation of the temporal and spatial nature has been notoriously difficult [*Lühr et al.*, 2015; *Stasiewicz et al.*, 2000]. Nevertheless, a vast amount of previous studies has been formed, based mainly on single spacecraft or indirect observations, since their first identification [*Zmuda et al.*, 1966, 1967; *Iijima and Potemra*, 1976]. Most studies have been forced to make assumptions of time stationarity (to apply *dB/dt* to a spatial estimate) or geometry (such as infinite sheets). At higher magnetospheric distances some multispacecraft analysis is possible [e.g., *Marchaudon et al.*, 2009; *Slavin et al.*, 2008], and indeed, the distributed multispacecraft capability of Active Magnetosphere and Planetary Electrodynamics Response Experiment [*Anderson et al.*, 2000], although limited in accuracy, is providing global features of FACs. Although statistical, multispacecraft studies have been performed previously [e.g., *Gjerloev et al.*, 2011], detailed resolution of individual FAC structure with close formations of spacecraft at both low- and medium-Earth orbits has not been performed until the advent of the multispacecraft Swarm and Cluster missions.

The three Swarm [*Friis-Christensen et al.*, 2008] spacecraft, named A, B, and C, were launched on 22 November 2013 and have been placed into phased, circular, low-Earth (LEO) polar orbits since the start of full science operations on 17 April 2014. Two spacecraft (A/C) are flying side by side at a mean high-latitude altitude of 481 km (during the time of the event), with orbital periods of ~94 min, while the third spacecraft (B) flies at a relatively drifting, slightly higher orbit at ~531 km altitude, with a slightly different orbital period of ~95 min. At the start of science operations the orbit planes were closely aligned so that the three spacecraft flew close to each other at times, where this close configuration repeats every few days. The polar orbits take the Swarm spacecraft through the auroral regions and across the polar cap at high

latitudes and sample all local times in about 132 days (spacecraft A/C), similar to the coverage of the CHAMP spacecraft [*Reigber et al*., 2002].

Cluster [*Escoubet et al*., 2001] has been operating since February 2001 and still has a fully operational complement of magnetometers [*Balogh et al*., 2001] and other instrumentation on all four spacecraft. At the start of the Swarm operations, the four Cluster spacecraft were flying in tilted, eccentric orbits, with perigee heights ranging between 3 and 4 R_E. For several hours around perigee, Cluster passes through the Earth's ring current and often passes through the region of high-latitude large-scale field aligned currents (FACs) above and below the ring plane (magnetic equator). The Swarm orbital planes drift relatively to Cluster at about 131 (spacecraft A/C) and 108 (spacecraft B) deg/yr so that the alignment with the Cluster orbit slowly changes throughout the mission. In order to enhance the coordination between the missions, the Cluster configuration was optimized to achieve the smallest and most compact configuration in the equatorial plane.

Here we explore one particular conjunction using multispacecraft analysis (adapting the methods of *Dunlop et al*. [1988, 2002], *Ritter and Lühr* [2006], and *Ritter et al*. [2013]), which assists the identification of the current signatures in each data set. We also employ a recently developed method [*Xiong et al*., 2014; *Xiong and Lühr*, 2014] to identify crossings of the expected poleward and equatorward auroral boundaries (taken as the maximum gradient in R1 and R2 FAC power) and employ their statistical model of the form of these boundaries (derived from small- and medium-scale FACs using 10 years of CHAMP magnetic field data) to help order both data sets.

2. Methodology

We use spin averaged data from the fluxgate magnetometers (FGM) onboard Cluster [*Balogh et al*., 2001] and 1 Hz level 1b data (https://earth.esa.int/web/guest/swarm/data-access) from the Vector Fluxgate Magnetometers (VFM) [*Friis-Christensen et al*., 2008] on Swarm. The orbits of the spacecraft from both missions in principle allow spatial gradient estimates of magnetic field measurements to be made. Depending on the spacecraft configuration, the four Cluster spacecraft allow a direct calculation of the curl of the magnetic field, thereby providing an estimate of all components of the electric current density [*Dunlop et al*., 1988, 2002; *Robert et al*., 1998]. The three Swarm spacecraft, even when flying in close formation, allow only a partial estimate of the current density (i.e., one component, normal to the plane of the configuration, see also *Shen et al*. [2012] and *Vogt and Marghitu* [2009]), unless the magnetic field is assumed to be stationary. In particular, if the magnetic field is assumed not to vary on short time scales of a few up to 20 s at LEO and is suitably filtered, then adjacent (time shifted) positions of the spacecraft can add to the number of spatial positions used to estimate the differences in the magnetic field between each position ([see *Ritter and Lühr*, 2006] as applied to the A-C low pair of Swarm spacecraft flying side by side for calculation of filed-aligned current). Here we apply a generalization of this methodology to produce two-, three-, and four-point spacecraft estimates of current density from the basic three-point spacecraft spatial configuration of Swarm.

In Figure 1a, the magnetic field values taken at the earlier times of the shifted positions A′ and C″ combined with those taken at the time of the A, B, and C positions provide a measurement set from up to five spatial points, from which the magnetic gradients (and curl B in particular) may be estimated (in principle, the position of B could also be time shifted). By selecting groups of three or four spacecraft (as well as using the spatial array ABC), a "curlometer" estimate can be made such that three spacecraft positions form one plane in Figure 1a, yielding the current density component normal to the plane, and four spacecraft form a tetrahedron, recovering the full curlometer estimate and yielding the full vector current density. In the case of four spacecraft the quality parameter from div B can also be estimated. The curlometer estimate provides a stable result point by point in time, and the quality of the estimate can be tracked by div B/curl B, for example. Clearly, if the three Swarm spacecraft are close together, as shown here, different tetrahedral configurations may be selected and the five positions provide some redundancy in the calculation. The stability and sensitivity of these methods will be described in a future paper; however, we find that the optimal time shift for this event was ~20 s.

Nevertheless, a number of points should be noted. First, for groups of three spacecraft, or nearly planar configurations (ACA′C′), only one current density component is found so that the field-aligned current is

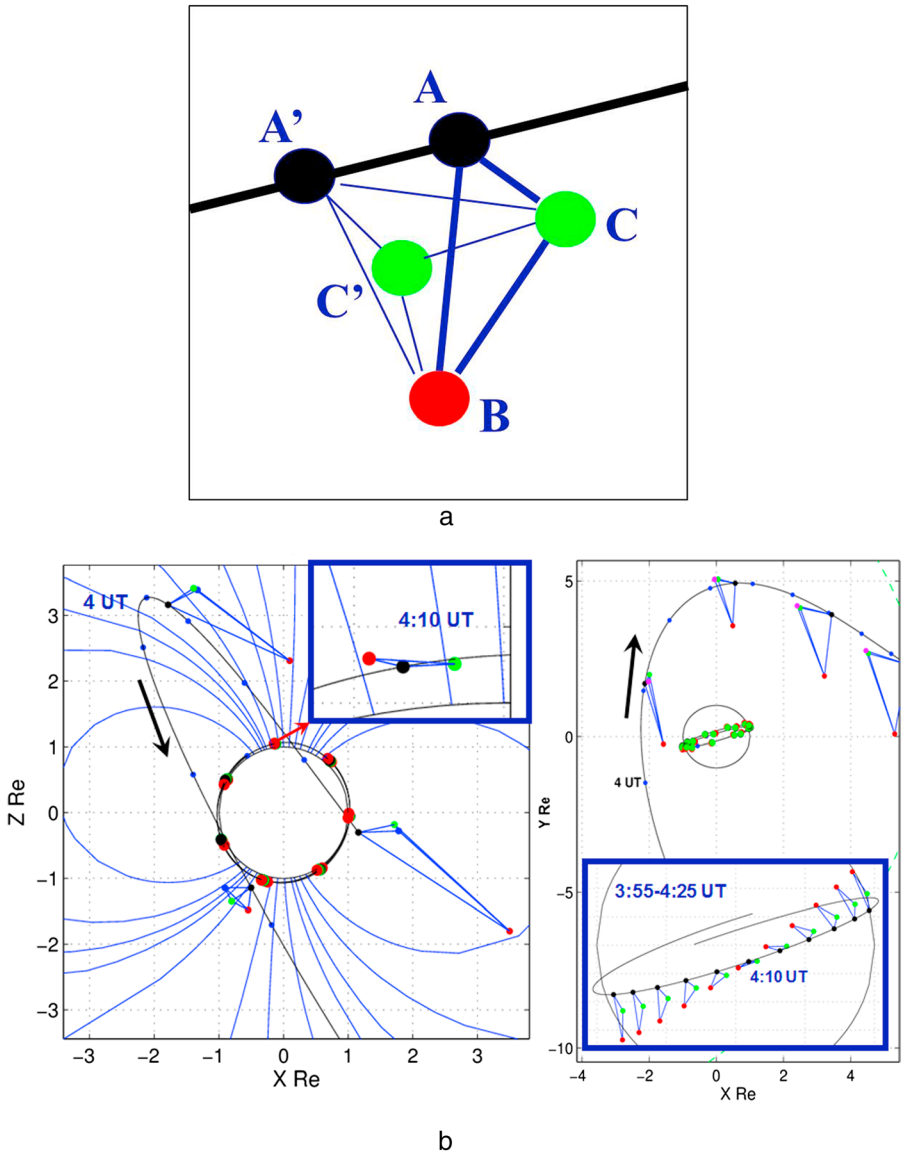

Figure 1. (a) Illustration of the multispacecraft technique as applied to Swarm measurements. The three Swarm spacecraft, A, B, and C are drawn relative to the orbit of Swarm A for a particular time. The positions A′ and C′ are positions at a slightly earlier time. For nominal operations, the spacecraft A and C fly side by side along similar orbits having slightly different local times (which crossover as the spacecraft fly over the poles). Swarm B is flying at a slightly higher altitude and in this example lags behind the A-C pair. (b): The orbits of Cluster and Swarm relative to the Earth in GSM coordinates on the 22 April 2014, projected into (left) Z,X_{GSM} and (right) Y,X_{GSM}. The Earth is shown as a circle with model geomagnetic field lines shown for guidance in the Z,X projection. The Cluster configurations are shown enlarged by a factor of 3 relative to the orbit track of C1. The insets show zoomed views of the Swarm spacecraft configurations, projected into each plane, enlarged by a factor of 5 relative to the orbit of Swarm A. The Cluster colors are: C1-black, C2-red, C3-green, and C4-blue, while the Swarm colors are A-black, B-red, and C-green.

only obtained from the projection of this component onto the field-aligned direction (this is true also for the standard Level 2 A-C data product in the Swarm data set [*Ritter et al.*, 2013], i.e., using the plane formed by AA′ CC′). Second, each group of spacecraft results in a current density estimate, which relates to a particular barycenter (center of volume of the configuration [see *Harvey*, 1998]) so that the combination of different groups of spacecraft refers to slightly different times, allowing the degree of stationarity of the measurement to be probed, in principle. For the configuration in Figure 1a, both four- and three-spacecraft estimates can be cross compared. The combination of Swarm A, B, and C produces a purely spatial estimate but forms a slightly tilted plane to the A, C orbit tracks (resulting in smaller-amplitude

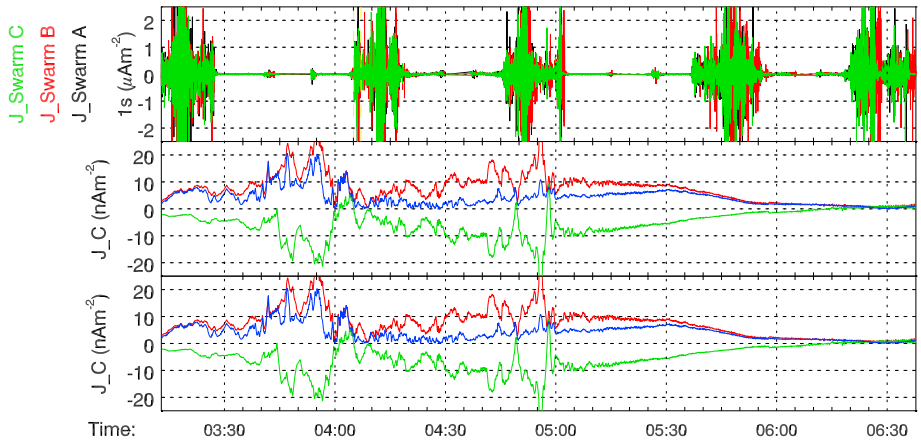

Figure 2. Plot of the FAC signatures seen by both Cluster and Swarm during the conjunction on 22 April 2014. (top) The estimate from Swarm data corresponding to the single spacecraft *dB*/*dt* for each of the three Swarm spacecraft [see *Xiong et al*., 2014]. The data are the Swarm Level 2 data set FAC_TMS_2F (available at https://earth.esa.int/web/guest/swarm/data-access) derived using VFM measurements [*Ritter et al*., 2013]. On Cluster, the current density is estimated via the curlometer technique for residual magnetic field data obtained by subtracting the International Geomagnetic Reference Field model. We have used (middle) the full four-spacecraft configuration and (bottom) the component of *J* normal to the face formed by C1, C3, and C4 (which is nearly aligned with the background magnetic field direction). The Swarm estimates are shown in black red and green (for A, B, and C). For Cluster in each case the total |*J*| (red trace), *J*perp (blue trace), and $J_{||}$ (cyan) are shown.

projections parallel to the field) and corresponds to the leading time of measurement (resulting in a small time shift in the signature). In the analysis below, these points should be borne in mind.

3. Event Analysis

On 22 April 2014 a close conjunction between the Cluster and Swarm arrays occurred. Figure 1b (right) shows that Cluster was flying from dawn to dusk through midnight local time during the few hours around 04:00 UT and passed from low to high invariant magnetic latitudes (MLAT) at around midnight local time, and at 2.5 R_E altitude, before falling again to low latitudes and passing through the magnetic equator (Figure 1b, left). During part of this interval (~03:55–04:25 UT), the Swarm spacecraft flew through the auroral zone and across the polar cap in a close configuration (~100–150 km separation) of all three spacecraft (see inset in Figure 1b (right)). For the period of interest here, the Cluster configurations were such that three spacecraft (C1, C3, and C4) were close together (~1000 km separation) and in a plane nearly perpendicular to the magnetospheric field, while the fourth spacecraft, C2-red, lay farther away (at ~5000 km separation from the others). The Swarm configurations show the crossover of the orbits just after 04:10 UT, and the inset in Figure 1b (left) also shows that Swarm and Cluster came into close magnetic alignment just before 04:10 UT where Swarm flew under the magnetic footprint of Cluster and shows the slightly higher altitude of the Swarm B spacecraft.

An overview of the current signatures is shown in Figure 2, for two Swarm orbits covering the interval of interest, where Swarm crosses first the southern then northern polar regions in each orbit. The Cluster estimates show that the FACs grow initially negative just after 03:45 UT and remain so until 04:00 UT, where $J_{||}$ turns slightly positive, and remains small until about 04:10 UT, when $J_{||}$ starts to grow again negative. A sharp change in $J_{||}$ occurs at around 04:55 UT.

Figure 3 shows the mapped orbits of both Swarm and Cluster (we use ground magnetic footprints, from Tsyganenko, T89 model [*Tsyganenko*, 1989], to obtain a stable, relative position) and confirms that the footprint of Swarm crosses the Cluster orbit footprint between 04:05 and 04:07 UT. The orbit tracks are plotted relative to fitted auroral boundaries. The latitudes of these equatorward and poleward boundaries both depend, but in different ways, on magnetic activity, forming well-defined ellipses around the magnetic poles, and expand with increasing activity. The basic shape is controlled by the dayside merging electric field, fitted statistically as ellipses to CHAMP data for different conditions by *Xiong et al*. [2014] and

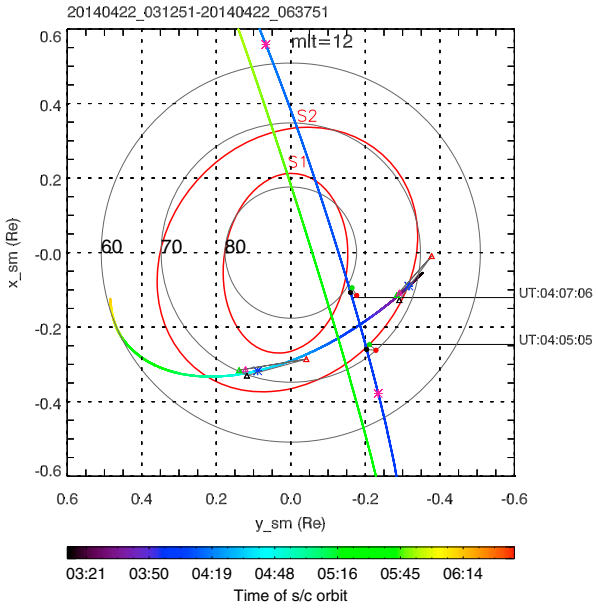

Figure 3. Mapped footprints of Cluster and Swarm (where two passes are shown) in SM coordinates on the 22 April 2014, together with model, equatorward and poleward, auroral boundaries, marked as S1 and S2 (referring to the expected locations of maximum R1 and R2 FA currents), which are taken from the fits in equation 8 of *Xiong and Lühr* [2014] after coordinate transformation. The times along the Swarm orbit for actual positions of the maximum gradients in FAC density (after *Xiong et al.* [2014]) are shown.

Xiong and Lühr [2014]. We plot the ellipses here for the times of the midpoints of the Swarm positions indicated by colored dots on the Swarm orbit (Cluster positions are indicated by triangles). The mapped locations for Cluster 1, 3, and 4 cover the same scale as the Swarm array, so that the FACs are approximately covered on the same relative scale at each location. The analysis of the FAC intensity, using the method of *Xiong et al.* [2014], has been directly applied to the Swarm data for this interval, where the times indicated along the right-hand Swarm track correspond to the actual estimates of the maximum gradient in FAC intensity.

The Cluster orbit is drawn from 03:40 to 05:00 UT, and both the Cluster and Swarm tracks are color coded with time. The orbits cross at about the same UT (Cluster crosses the magnetic local time (MLT) of Swarm a few minutes earlier than the Swarm flyover), and Cluster moves from lower (~70°) to higher (~75°) MLAT, and back to lower MLAT, as it moves across MLT. Cluster enters the region of negative parallel current, $J_{||}$, shown in Figure 2, as it approaches and crosses the S2 boundary just after 03:45 UT (at MLAT = 71°) and as it approaches the boundary again, crossing just after 04:55 UT and at MLAT = 67° (consistent with the connectivity of R2 large-scale currents for this dawn-side local time). At the higher MLAT = 75° positions, Cluster approaches the S1 boundary where it shows zero or positive $J_{||}$ (between ~04:00 and 04:15 UT).

Meanwhile, on the first northern track on the right, Swarm enters a region of FACs as it crosses the S2 boundary initially at 04:04 UT (MLAT = 71°), which continue over the pass and are broadly consistent with the expected S1 and S2 boundaries as drawn, although other current systems are present. This first northern Swarm pass therefore occurs just after Cluster reaches high latitudes, while the second period of negative $J_{||}$ on cluster occurs while Swarm is in the south. We therefore select the period 03:40–04:20 UT, which contains the first large-scale FAC at Cluster and the northern pass of Swarm, for detailed analysis. We refer below to large-scale and small-scale FACs to correspond to scale sizes at Swarm altitudes of $>$150 km and $<$150 km, respectively.

Figure 4 shows more detailed estimates of the currents seen by Swarm using one-, two-, three-, and four-spacecraft calculations from the configurations shown in Figure 1b and as constructed from the time shift methods described in section 2. The lower set of panels show the whole northern pass of Swarm, as shown in Figure 2 (but over the core time interval 04:03–04:19 UT), while the inset (upper graphs) show the first short burst of FACs on Swarm (during which Swarm crosses the Cluster orbit), containing the ascending crossings of the S1/S2 boundaries (as indicated), which have been determined from the position of maximum gradients in FAC power. It can be seen from Figure 2 that these crossings correspond to the model boundary position for S2 and near the position of the S1 boundary. The other vertical lines in the lower set of panels are drawn to mark the different positions along the Swarm orbit, where the dashed line at 04:11 UT corresponds to the position of the A/C and B orbit crossover (as indicated in Figure 1b), while the A, C spacecraft cross at 04:12:30 UT. The last vertical line at 04:14 UT can be seen to correspond to the first drop in size of the FACs and corresponds to the descending position of the S2 oval as drawn on Figure 2.

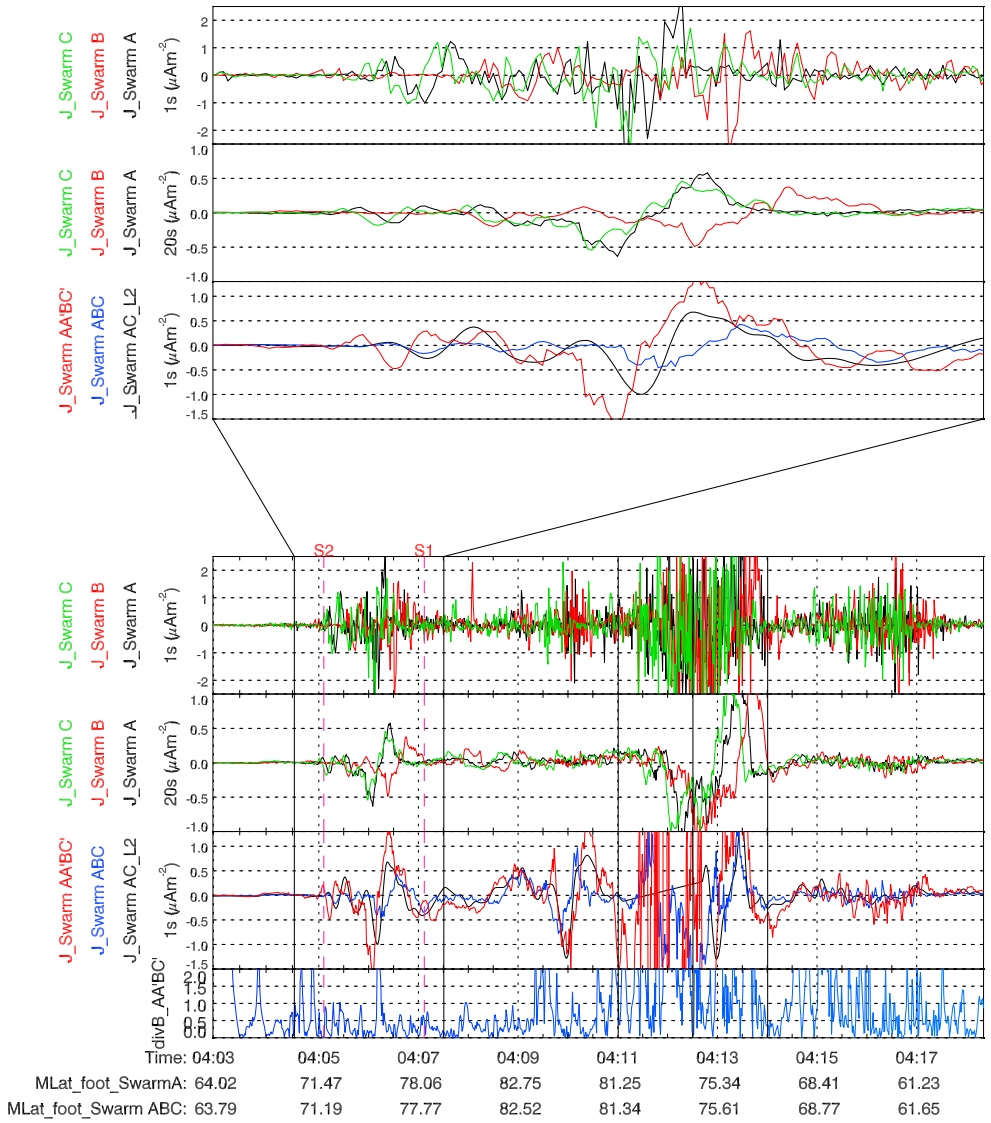

Figure 4. The FAC estimates for Swarm for the whole northern pass (lower set) and the intervals containing (top set) the ascending S2, S1 crossings. In each set, the three panels represent (from the top): (first panel) the single-spacecraft estimates from *dB/dt*; (second panel) the filtered single-spacecraft estimates (20 s window), and (third panel) the two-, three-, and four-spacecraft curlometer estimates. For the estimates in the lower set of each set, we have applied the analysis to residual magnetic field data obtained by subtracting the CHAOS-4plus model [e.g., *Olsen et al.*, 2014]. We have additionally shown the ratios of div B/curl B obtained with the four-spacecraft estimate in the lowest panel. This shows low values (high quality) for the key intervals containing the FACs.

The FAC estimates are best seen in the top set of panels. Here the top two panels show single-spacecraft signatures, which have similar, time shifted profiles corresponding to the relative positions of spacecraft A, B, and C as they cross the region: Swarm A and C are almost side by side, while Swarm B lags behind (~25 s). It is also apparent that Swarm B, at a slightly higher altitude, sees a lower amplitude signature, particularly in the filtered trace. The third panel shows the smoothed, time shifted calculation for the pair of A/C spacecraft (after *Ritter et al.* [2013]) in black, the full four time-shifted spacecraft curlometer estimate in red, and the three-spacecraft estimate from A, B, and C configuration (in blue). Note that the three-spacecraft estimate provides the *J* normal to the ABC plane, which is tilted with respect to the FACs, so that the FA projection has a lower amplitude to that of the four-point estimate of the parallel component of the full current density vector, **J**. The signatures of each estimate in the third panel are similar but are also time shifted since the barycenter, and hence effective time, of the estimate is slightly

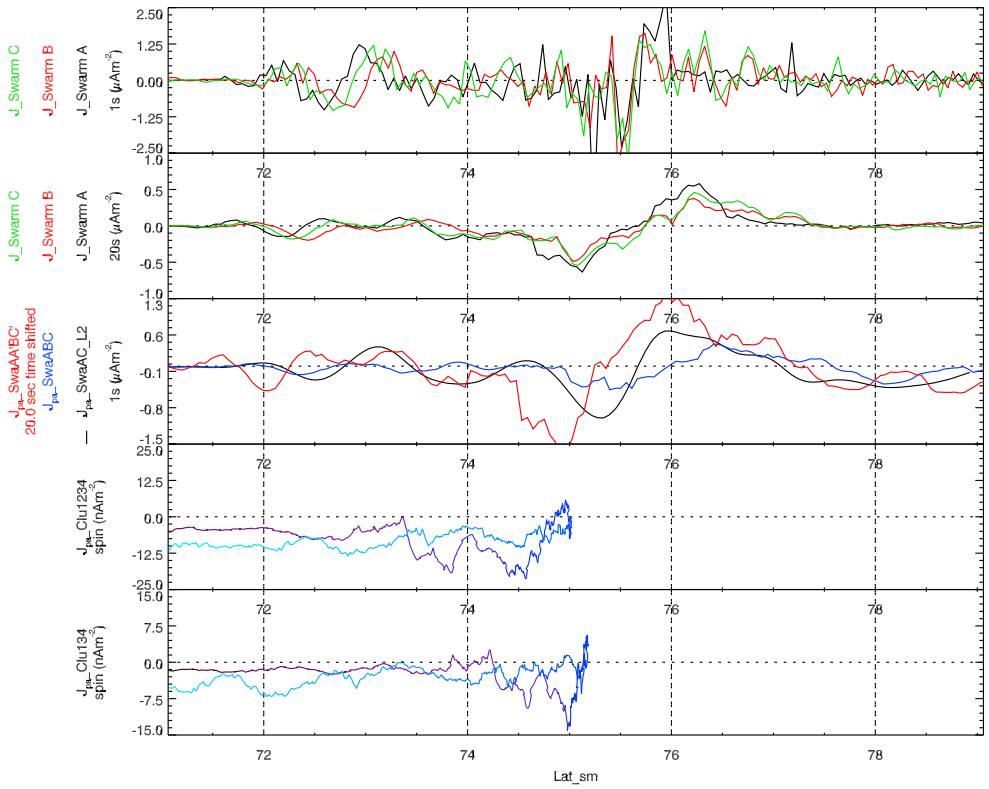

Figure 5. Mapped MLAT (in SM coordinates) values of Swarm and Cluster FACs. The top three panels correspond to the same set of FAC estimates as shown in the top set of panels in Figure 5. The bottom two panels show the Cluster FACs estimated by the full curlometer and from one face formed by C1, C3, and C4 (as in the bottom two panels of Figure 4).

different for each. In the lower set of panels it can be seen that the larger-scale features are better revealed by the filtered single-spacecraft estimates; however, the three- and four-spacecraft estimates also provide values throughout the interval, and although similar, there are differences in detail between the estimates.

In order to track and compare these FAC features to those seen at Cluster, in Figure 5 we plot the Swarm and Cluster signatures in terms of their MLAT position. The Swarm plot corresponds to the time interval ~04:05–04:07:30 UT, which contains the FACs seen between the S1 and S2 boundaries, while Cluster is plotted for the whole interval as it moves from MLAT = 71° and back again (03:30–04:40 UT). In this comparison it needs to be borne in mind that there is a MLT difference between Cluster and Swarm, which develops through the interval. Nevertheless, it can be seen that there are distinct features which appear. For Swarm, we see that the single-spacecraft estimates contain two clear time-independent signatures. The first is a large-scale (compared to the separation of the Swarm Satellites, i.e., approximately 150 km) feature between MLAT = 74° and 76° since it is sampled at the same position by each spacecraft as it flies through. The amplitude at the height of Swarm B is slightly reduced. The second (MLAT = 72° and 73°) is a small-scale structure since it is sampled at different MLAT positions by each spacecraft, implying limited (longitudinal) extent on the scale of the spacecraft separation.

For the multispacecraft analysis in the third panel, it can be seen that the three-spacecraft Swarm estimates derived from the ABC configuration (blue trace) broadly agree with the Swarm B signature in the second panel, while the four-spacecraft curlometer (red trace) show a more pronounced signature (since it is derived from the full vector current estimate). Note that since the barycenters of the multispacecraft estimates differ slightly, there is no exact correspondence in MLAT. The Cluster traces show the signatures as the Cluster array moves from 71° to 75° (dark blue trace) and then back to 71° (light blue trace). The dark blue trace corresponds most closely in time with Swarm between 74° and 75° and shows a very similar profile in MLAT to the four-spacecraft estimate from Swarm (red trace, third panel). The two Cluster estimates (from four-and three-spacecraft calculations) serve to show the change in the effective location

of the measurement (the configurations in Figure 1b show that spacecraft C2 significantly shifts the effective mean position of Cluster). Nevertheless, the profiles show a remarkable similarity to Swarm and at similar MLAT positions, allowing for the slight shift in MLT between the spacecraft arrays. It is therefore probable that Cluster is sampling the same large-scale FAC as Swarm. The amplitudes of the FAC are also consistent: based on the expansion of the field lines, the FA current sheet cross section should scale by about a factor of ~60 between the Swarm and Cluster altitudes. We find that the amplitudes of current densities at Swarm and Cluster are ~1.3 μAm^{-2} and 20 nAm^{-2}, respectively, giving a ratio of ~65. We would not expect the small-scale structure seen by Swarm at 73° to map to Cluster positions in any coherent manner, and indeed, there is no clear signature seen by Cluster at this position.

4. Conclusion

We have analyzed a close magnetic conjunction between the Swarm and Cluster spacecraft arrays, where three Swarm spacecraft are flying in close formation and the Cluster configuration is elongated but is well aligned to the background magnetic field direction. This data set therefore allows detailed, multispacecraft analysis of the magnetic field measurements at both the Swarm and Cluster locations. We have therefore been able to identify for the first time at low (~500 km altitude) Earth orbit (just above the typical F_2 peak of the ionosphere) the spatial form of the field-aligned current density and have been able to match these signatures to those seen at Cluster (located at higher altitudes ~3.5 R_E from Earth center) in the magnetosphere. The Cluster signatures are interpreted and ordered through joint mapping of the ground magnetospheric footprints and estimation of the auroral zone boundaries (taken as indication of the boundaries of Region 1 and Region 2 currents). We find clear evidence of both small-scale and large-scale FACs, and clear matching of the behavior and structure of the large-scale currents at both Cluster and Swarm. The methodology is made possible through the joint operations of Cluster and Swarm, which contain, in the first several months of Swarm operations, a number of close three-spacecraft configurations. The analysis has been performed by adapting the curlometer technique to the configurations and magnetic environment at Swarm, and the comparison of C1, C2, C3, and C4 point analysis has allowed the separation of temporal and spatial behavior to be probed to some degree. In addition, the four-spacecraft technique allows an estimate of all components of the current density to be made, so that perpendicular current signatures may also be investigated alongside the field-aligned currents. This allows the Hall current signatures to be investigated directly and will be the subject of future work.

Acknowledgments

We thank the ESA Swarm project for provision of the data used here. This work is supported by the NSFC grants 41174141, 41431071, and 40904042; 973 program 2011CB811404; and NERC grant NE/H004076/1. M.W.D. is partly supported by STFC in-house research grant. Y.Y.Y. is sponsored by China State Scholarship Fund (201404910456) to visit at RAL. We would like to thank T. Oddy at Imperial College for helping with the provision of Cluster FGM data.

The Editor thanks Colin Waters and an anonymous reviewer for their assistance in evaluating this paper.

References

Anderson, B. J., K. Takahashi, and B. A. Toth (2000), Sensing Global Birkeland currents with Iridium engineering magnetometer data, *Geophys. Res. Lett.*, *27*, 4045–4048, doi:10.1029/2000GL000094.

Balogh, A., et al. (2001), The Cluster Magnetic Field Investigation: Overview of in-flight performance and initial results, *Ann. Geophys.*, *19*, 1207–1218.

Cao, J.-B., et al. (2010), Geomagnetic signatures of current wedge produced by fast flows in a plasma sheet, *J. Geophys. Res.*, *115*, A08205, doi:10.1029/2009JA014891.

Dunlop, M. W., D. J. Southwood, K.-H. Glassmeier, and F. M. Neubauer (1988), Analysis of multipoint magnetometer data, *Adv. Space Res.*, *8*, 273–277.

Dunlop, M. W., A. Balogh, K.-H. Glassmeier, and the FGM team (2002), Four-point Cluster application of magnetic field analysis tools: The curlometer, *J. Geophys. Res.*, *107*(A11), 1385, doi:10.1029/2001JA005089.

Escoubet, C. P., M. Fehringer, and M. Goldstein (2001), Introduction: The Cluster mission, *Ann. Geophys.*, *19*, 1197–1200.

Friis-Christensen, E., H. Lühr, D. Knudsen, and R. Haagmans (2008), Swarm – An Earth observation mission investigating Geospace, *Adv. Space Res.*, *41*, 210–216, doi:10.1016/j.asr.2006.10.008.

Gjerloev, J. W., S. Ohtani, T. Iijima, B. Anderson, J. Slavin, and G. Le (2011), Characteristics of the terrestrial field-aligned current system, *Ann. Geophys.*, *29*, 1713–1729, doi:10.5194/angeo-29-1713-2011.

Harvey, C. C. (1998), Spatial gradients and the volumetric tensor, in *Analysis Methods for Multi-Spacecraft Data*, ISSI Sci. Rep., SR-001, edited by G. Paschmann and P. W. Daly, pp. 307, Kluwer Acad., Dordrecht, Netherlands.

Iijima, T., and T. A. Potemra (1976), The amplitude distribution of field aligned currents at northern high latitudes observed by Triad, *J. Geophys. Res.*, *81*, 2165–2174, doi:10.1029/JA081i013p02165.

Lühr, H., J. Park, J. W. Gjerloev, J. Rauberg, I. Michaelis, J. M. G. Merayo, and P. Brauer (2015), Field-aligned currents' scale analysis performed with the Swarm constellation, *Geophys. Res. Lett.*, *42*, 1–8, doi:10.1002/2014GL062453.

Marchaudon, A., J.-C. Cerisier, M. W. Dunlop, F. Pitout, J.-M. Bosqued, and A. N. Fazakerley (2009), Shape, size, velocity and field-aligned currents of dayside plasma injections: A multi-altitude study, *Ann. Geophys.*, *27*, 1251–1266, doi:10.5194/angeo-27-1251-2009.

McPherron, R. L., C. T. Russell, and M. P. Aubry (1973), Satellite studies of magnetospheric substorms on August 15, 1968: 9. Phenomenological model for substorms, *J. Geophys. Res.*, *78*(16), 3131–3149, doi:10.1029/JA078i016p03131.

Olsen, N., H. Lühr, C. C. Finlay, T. J. Sabaka, I. Michaelis, J. Rauberg, and L. Tøffner-Clausen (2014), The CHAOS-4 geomagnetic field model, *Geophys. J. Int.*, *197*, 815–827, doi:10.1093/gji/ggu033.

Reigber, C., H. Lühr, and P. Schwintzer (2002), CHAMP mission status, *Adv. Space Res.*, *30*(2), 129–134.

Ritter, P., and H. Lühr (2006), Curl-B technique applied to Swarm constellation for determining field-aligned currents, *Earth Planets Space*, *58*, 463–476.

Ritter, P., H. Lühr, and J. Rauberg (2013), Determining field-aligned currents with the Swarm constellation mission, *Earth Planets Space*, *65*, 1285–1294, doi:10.5047/eps.2013.09.006.

Robert, P., M. W. Dunlop, A. Roux, and G. Chanteur (1998), Accuracy of current density determination, in *Analysis Methods for Multispacecraft Data*, ISSI Sci. Rep., SR-001, Kluwer Acad., Dordrecht, Netherlands.

Shen, C., J. Rong, M. Dunlop, Y. H. Ma, G. Zeng, and Z. X. Liu (2012), Spatial gradients from irregular, multiple-point spacecraft configurations, *J. Geophys. Res.*, *117*, A11207, doi:10.1029/2012JA018075.

Shiokawa, K., et al. (1998), High-speed ion flow, substorm current wedge and multiple Pi2 pulsations, *J. Geophys. Res.*, *103*(A3), 4491–4507, doi:10.1029/97JA01680.

Slavin, J. A., G. Le, R. J. Strangeway, Y. Wang, S. A. Boardsen, M. B. Moldwin, and H. E. Spence (2008), Space technology 5 multipoint measurements of near-Earth magnetic fields: Initial results, *Geophys. Res. Lett.*, *35*, L02107, doi:10.1029/2007GL031728.

Stasiewicz, K., et al. (2000), Small-scale Alfvénic structure in the aurora, *Space Sci. Rev.*, *92*, 423–533, doi:10.1023/A:1005207202143.

Tsyganenko, N. A. (1989), A magnetospheric magnetic field model with a warped tail current sheet, *Planet. Space Sci.*, *37*, 5–20.

Vogt, J., and O. Marghitu (2009), Analysis of three-spacecraft data using planar reciprocal vectors: Methodological framework and spatial gradient estimation, *Ann. Geophys.*, *27*, 3249–3273, doi:10.5194/angeo-27-3249-2009.

Xiong, C., and H. Lühr (2014), An empirical model of the auroral oval derived from CHAMP field-aligned current signatures – Part 2, *Ann. Geophys.*, *32*, 623–631, doi:10.5194/angeo-32-623-2014.

Xiong, C., H. Lühr, H. Wang, and M. G. Johnsen (2014), Determining the boundaries of the auroral oval from CHAMP field-aligned currents signatures – Part 1, *Ann. Geophys.*, *32*, 609–622, doi:10.5194/angeo-32-609-2014.

Zmuda, A. J., J. H. Martin, and F. T. Heuring (1966), Transverse magnetic disturbances at 1100 kilometers in the auroral region, *J. Geophys. Res.*, *71*, 5033–5045, doi:10.1029/JZ071i021p05033.

Zmuda, A. J., F. T. Heuring, and J. H. Martin (1967), Dayside magnetic disturbances at 1100 kilometers in the auroral oval, *J. Geophys. Res.*, *72*, 1115–1117, doi:10.1029/JZ072i003p01115.